

RESEARCH ARTICLE

Remote Sensing for Sustainable Oceans
2025, Vol. 00(00) 1-12
DOI: [10.47852/bonviewRSSO52026073](https://doi.org/10.47852/bonviewRSSO52026073)

NDWI–NDBI Overlay–Based Analysis of Coastal Fence Expansion and Hydrological Changes in Victoria Island, Lagos, Nigeria (2010–2015), with Machine Learning Validation

Inuwa Sani Sani^{1,*}, Parluhutan Manurung¹ and Anas Usman Fagge²¹ Department of Geography, Universitas Indonesia, Indonesia² Department of Geography, Sa'adatu Rimi College of Education, Nigeria

Abstract: Coastal ecosystems are becoming increasingly susceptible to anthropogenic impact and the process of infrastructure construction, particularly within fast-urbanizing zones. This study examines the spatiotemporal processes of coastal fence growth and surface water loss during 2010–2015 in Victoria Island, Lagos. Landsat imagery was employed in extracting the Normalized Difference Water Index (NDWI) and the Normalized Difference Built-up Index (NDBI), the former being the prime indicator of hydrological alteration, while the latter being the key indicator of urban growth. NDWI loss areas coincide with NDBI gain areas to identify areas where natural water bodies are substituted by artificial structures in the guise of coastal fences. Supervised machine learning–based classification was employed for improved change detection and spatial precision. This study introduces a new application of NDWI–NDBI overlay and supervised machine learning to coastal fencing identification in Lagos, Nigeria, and the approach provides a reproducible model for monitoring structural change in coastal communities that have limited data. The result clearly demonstrates that the reduction in the extent of surface water has a strong correlation with the expansion of built-up land, particularly along the coasts, where coastal fences have been extended seaward. This study demonstrates the application of fused spectral indices and machine learning to monitor coastal change and offers a reproducible technique for sustainable coastal zone management.

Keywords: machine learning, Victoria Island, Lagos, coastal fence, NDWI, NDBI

1. Introduction

The coastline is an interface where three basic natural systems converge: the atmosphere, land ecosystems, and bodies of water, and it is made up of diverse ecosystem services that are increasingly susceptible to both natural processes and human activities, particularly those related to climate change [1]. Coastal ecosystems are some of the most dynamic and biologically productive environments on our planet, where the terrestrial and marine worlds overlap and act as interfaces [2]. The coastal zones are densely endowed with diverse ecosystems and are the locations of key economic activities while being exposed to increased vulnerability through urbanization, human settlements, and global phenomena such as sea level rise and beach erosion [3]. In all developing nations such as Nigeria, human activities such as the building of seawalls, groins, and fencing walls have altered the natural process of the coast [4].

Coastal cities are aggressively being redeveloped by natural and human forces like population expansion, economic growth, and climatically induced environmental modification. Nowhere is such change more acute than in the world's megacities, like Lagos, Nigeria, where coastal reclamations and uncontrolled urban sprawl have diverted natural hydrologic flows and coastlines.

Victoria Island, one of the most rapidly developing Lagos coastal suburbs in Nigeria, is a good example situated in the Atlantic Ocean and driven by its economic opportunities; the suburb has undergone extensive land reclamation, infrastructural development, and shoreline modification, such as the construction of coastal fences [5].

This study utilizes Landsat 7 ETM+ imagery (2010–2015) due to its optimal compromise between spatial resolution (30m), temporal continuity, and free-access availability during the study period. Although the more recent imagery like Sentinel-2 (10m) or MODIS is ideal, their availability started after 2015, so Landsat 7 was selected due to (1) the archive fully spanning our period of study (available before the start of Sentinel-2 in 2015), (2) the 30m resolution being adequate for distinguishing coastal fencing regimes while permitting practical multi-year processing, and (3) the properly calibrated ETM+ sensor generating standard surface reflectance data of greatest usefulness in inferring incremental shoreline change. That homogeneity is required for tracking human-induced fine-scale changes within data-scarce regions. Although fences are typically constructed for flood protection or marking land boundaries, they have extensive environmental and spatial ramifications on the coastal environment.

Satellite remote sensing has proven to be a vital tool for monitoring such change with temporal continuity and over broad spatial extents. There are several different classification methods used for satellite land use/land cover change detection. These include supervised machine learning classifiers (Support Vector Machine, Random Forest [RF]),

*Corresponding author: Inuwa Sani Sani, Department of Geography, Universitas Indonesia, Indonesia. Email: inuwa.sani@ui.ac.id

unsupervised classification (K-means clustering), object-based image analysis, and index-based threshold classification. While supervised classification methods are more precise when ground truth information is provided, threshold-based classification methods are simpler to interpret, computationally faster, and suitable for index-specific studies.

In this study, the term “fence” refers to man-made physical barriers or obstructions such as solid walls, embankments, or enclosures that are constructed along a seashore or in water bodies for the sake of land marking, reclamation, or development control. These fences most commonly lead to urbanization of developed land intruding coastal or water areas, typically replacing natural water surface with impervious cover. While locally referred to as “coastal fences,” these are also regarded as illegal land reclamation or unofficial shoreline hardening in international coastal terminology [6].

This study follows two spectral indices: Normalized Difference Water Index (NDWI) and Normalized Difference Built-up Index (NDBI), for monitoring coastal dynamics and mapping fencing-induced change in Victoria Island in 2010–2015. NDWI, based on green and near-infrared (NIR) reflectance, was demonstrated to be suitable for monitoring vegetation and surface water change [7], while NDBI, based on the short-wave infrared (SWIR) and NIR bands, was widely applied to estimate urban growth and built-up density. The use of these indices together enables the assessment of natural (water-induced) and anthropogenic (urban development) changes in the coastal zone at the same time.

This study utilizes a thresholding technique of NDWI (to identify water loss) and NDBI (to identify built-up growth) and meshes their opposing strengths to identify coastal fencing encroachment. While “NDWI=” $\frac{\text{Green} - \text{NIR}}{\text{Green} + \text{NIR}}$ identifies changes in surface water, “NDBI=” $\frac{\text{SWIR} - \text{NIR}}{\text{SWIR} + \text{NIR}}$ clearly maps urbanization patterns. Their intersection indicates water loss augmented with built-up gain a characteristic of coastal fencing. This two-index approach, which was verified by supervised machine learning (RF), addresses a fundamental knowledge deficit of West African urban coastal surveillance whereby such structural change is incremental but ecologically meaningful [8]. This study offers an extensible method for the detection of change in urbanizing coastlines and is aimed at filling this gap by leveraging multitemporal Landsat imagery and cloud-based geospatial processing platforms such as Google Earth Engine (GEE) and Google Colab to (1) quantify NDWI-based surface water change, (2) recognize NDBI-based structural development, and (3) establish spatial coincidences of possible coastal fencing.

The objective of this research is to examine the spreading of coastal fences in Victoria Island, Lagos, Nigeria, in 2010–2015. Through the application of threshold values of NDWI and NDBI on Landsat data, we identify water loss patches with an attendant increase in built-up land, an indication of reclamation or structural fencing. The result will inform evidence-based policymaking and coastal management for risky urban coasts.

2. Literature Review

Shoreline land cover change monitoring requires discrimination indices between urbanized and hydrological features. NDWI has also been highly applied in the identification of surface water bodies and changes, especially for areas that have shoreline recession or anthropogenic alteration [9]. NDWI is also highly useful in the identification of moisture content and water versus vegetation and soil and therefore highly useful in the identification of water loss trends and encroachment in the coastal region, or NDBI can often be utilized to extract built-up features using SWIR to NIR spectral contrast [10]. NDBI can effectively demarcate the extent of impervious cover and

infrastructure development, especially where human construction such as coastal fences or embankments is undertaken to reclaim land or to mitigate erosion in areas of the coastline that are prone to urbanization of the coast [11].

The integrated NDWI–NDBI overlay technique has recently been used to analyze anthropogenic stress on coastal regions. For instance, multi-index remote sensing applied with the intention of monitoring shoreline change and building intrusions along the affected coastal stretches by overlaying loss in NDWI and gain in NDBI has successfully found locations where natural water systems are being substituted by development and this method has been of invaluable use in the detection of illicit developments like coastal fencing, which is prone to intruding into intertidal or riparian zones [12].

Geospatially, Dike et al. [13] conducted a comparative analysis of shoreline demarcation in Nigeria with Landsat-8, Sentinel-2, and Planet Scope imagery and concluded that NDWI always outcompeted all other hydrological change mapping indices of coastal barriers. Likewise, it highlighted the importance of composite remote sensing indices in semi-arid tropical regions with increased utilization of high-spatial resolution, free-access imagery in successful land water interaction observation.

Despite progress, many studies have analyzed either hydrological or urban indices in isolation. Fewer have analyzed the spatial interaction between NDWI loss and NDBI gain in terms of coastal fencing and policy enforcement. This study tries to fill the gap by using multi-year Landsat imagery to detect coastal fence expansion in Victoria Island, Lagos, by applying NDWI and NDBI overlays to spatially depict the spatiotemporal interaction between built-up expansion and hydrological degradation.

3. Research Methodology

3.1. Study area

The Victoria Island was analyzed in a Lagos coastline as shown in Figure 1, geographically situated in the Atlantic Ocean in the south and the Lagos Lagoon to the north, and it is located between 6.412°N and 6.438°N latitude and 3.410°E and 3.450°E longitude [14]. Victoria Island is a fast-developing urban city consisting of business high-rise buildings, residential housing estates, and a huge seaside reclaimed area [15]. Its strategic and economic value has caused it to become a focus for coastal infrastructural investment, generally at the expense of natural habitats.

For performing the geospatial analysis, Victoria Island spatial extent was delineated from a high-resolution satellite image polygon shapefile and loaded as an asset in GEE to enable homogenous spatial filtering, masking, and visualization.

3.2. Data acquisition

Landsat 7 Enhanced Thematic Mapper Plus (ETM+) surface reflectance data were downloaded from the USGS Earth Explorer and GEE data archive, and data between 2010 and 2015 were used as shown in Figure 2. To prevent inconsistencies and less atmospheric deformation, images with coverage less than 30% were used separately and the median reducer was used to create yearly composites to mosaic cloud-free appearance yearly [16].

Table 1 presents NDWI (green and NIR bands) and NDBI (SWIR1 and NIR bands) analysis from Landsat 7 ETM+ imagery at 30m resolution, ensuring consistent water and built-up area assessment in 2010–2015.

Figure 1
Map of the study area

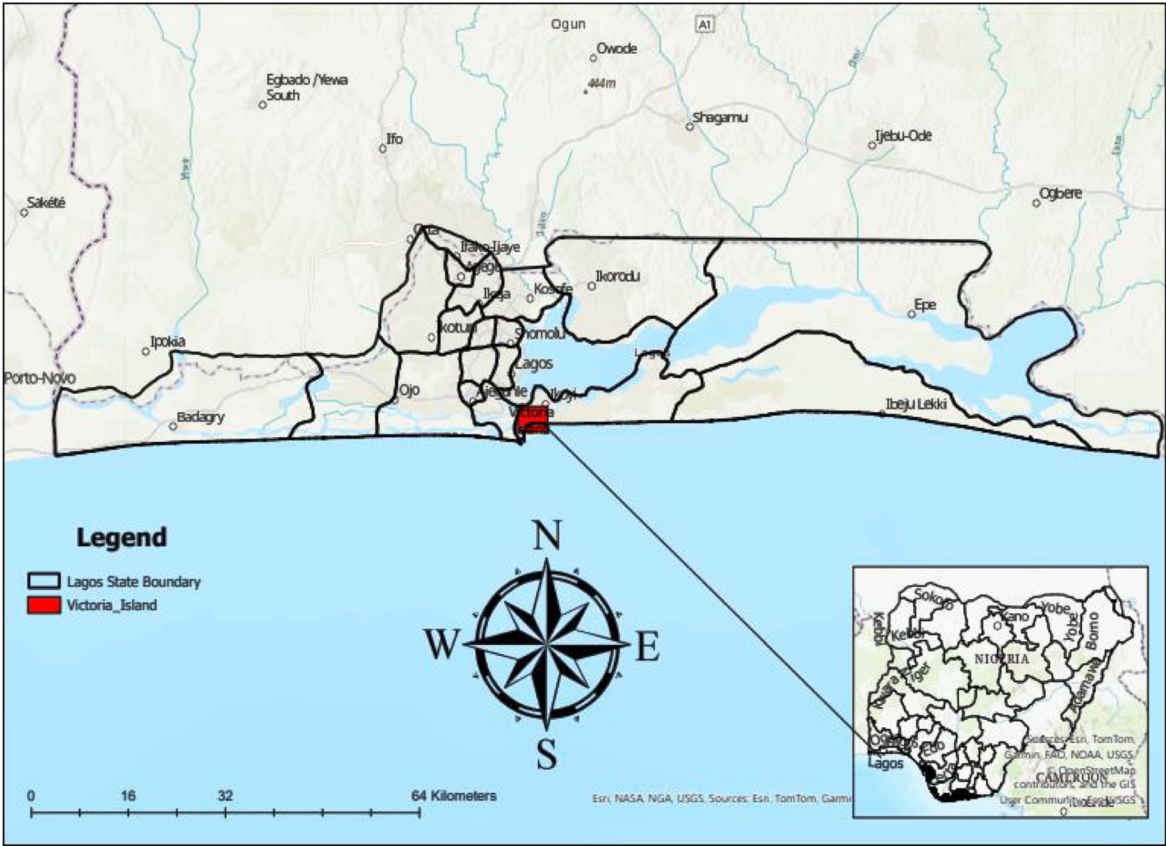
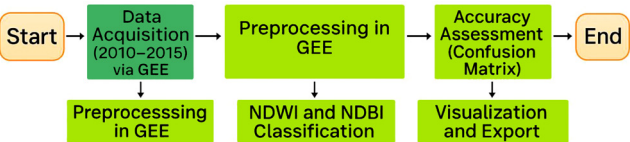


Figure 2
Coastal fence detection workflow



3.3. NDWI and NDBI computation

For successful observation and study of surface and built-up water flow patterns over the decades, two remote sensing indices were computed every year and the indices are of extremely important use in land use and hydrological trend studies, particularly for nations with rapid urbanization [17].

NDWI is one of the most popular indices utilized in surface water body detection and monitoring; the index utilizes the distinction between NIR and green satellite image bands in emphasizing water objects and the index differentiates best between water and other land classes and is hence reliable to measure the extent of surface water with time [18].

At the same time, the NDBI tries to distinguish built-up features from the difference between the subtraction of the SWIR and NIR bands. It is applied in the distinction of the urban development pattern and built-up expansion, and it is utilized in the management and planning of cities [19].

With its annual submission, researchers can monitor urban land and surface water patterns and observe how hydrological processes are impacted by urbanization and it allows them to investigate inter-annual fluctuation and long-term trend, a value that is of unthinkably crucial

Table 1
NDWI–NDBI analysis using Landsat data (2010–2015)

Year	Satellite	Sensor	Bands for NDWI	Bands for NDBI	Spatial resolution	Remarks
2010	Landsat 7	ETM+	Green (SR_B2), NIR (SR_B4)	SWIR1 (SR_B5), NIR (SR_B4)	30m	Minimal cloud cover
2011	Landsat 7	ETM+	Green (SR_B2), NIR (SR_B4)	SWIR1 (SR_B5), NIR (SR_B4)	30m	Stable data availability
2012	Landsat 7	ETM+	Green (SR_B2), NIR (SR_B4)	SWIR1 (SR_B5), NIR (SR_B4)	30m	Consistent quality
2013	Landsat 7	ETM+	Green (SR_B2), NIR (SR_B4)	SWIR1 (SR_B5), NIR (SR_B4)	30m	Used for change detection
2014	Landsat 7	ETM+	Green (SR_B2), NIR (SR_B4)	SWIR1 (SR_B5), NIR (SR_B4)	30m	Pre-fence expansion period
2015	Landsat 7	ETM+	Green (SR_B2), NIR (SR_B4)	SWIR1 (SR_B5), NIR (SR_B4)	30m	End of study period

significance in the sustainable development and resource management of the affected area. Both were computed as follows:

$$NDWI = \frac{Green - NIR}{Green + NIR}$$

This index enhances open water features while suppressing built-up and vegetation areas [20].

$$NDBI = \frac{SWIR - NIR}{SWIR + NIR}$$

This index highlights impervious surfaces and built-up structures [21].

Both indices were computed for each year from 2010 to 2015, and change detection was performed by calculating differences between consecutive years such as 2010–2011 and 2011–2012.

3.4. Threshold-based classification technique

For hydrological and urbanized change area mapping, we used threshold-based classification on the NDWI and NDBI indices. This was due to simplicity, readability, and where thematic classes are distinctly separated with discrete index values. Thresholding was also a computationally more efficient substitute for supervised classification methods based on tagged training samples. Thresholding can be simply replicated across time series satellite images [22].

NDWI was calculated from the NIR and green bands of the Landsat data, and NDBI was calculated from the SWIR and NIR bands. Based on literature and empirical verification, pixels with NDWI less than -0.1 were classified as water loss and pixels with NDBI higher than 0.1 were classified as built-up or new development [10]. These threshold values were established through iterative visual verification and validation using high-resolution Google Earth imagery by year.

These function-based thresholds perform optimally in coastal towns where surface water and impervious surface modification are spatially discrete and temporally rapid. Applying these thresholds to multitemporal 2010–2015 Landsat imagery, we generated binary layers of NDWI loss and NDBI gain, which were Spatially correlated for mapping patches of artificial fencing and coastal encroachment.

Thresholding, while not a machine learning method, was used as a baseline due to its simplicity, transparency, and computational efficiency. It involves applying fixed rule-based thresholds (NDWI < -0.1) to classify pixels and was evaluated against a RF model for comparative validation under data-limited conditions.

3.5. NDWI–NDBI overlay for detection of fencing

To find the locations where fencing or coastal reclamation was done, we created an overlay of the 2010 NDWI loss map and 2015 NDBI gain map. In this analysis, it identifies where water surfaces were lost (NDWI < -0.1) and replaced by man-made cover (NDBI > 0.1) at the same location between 2010 and 2015 satellite images. This overlap of these two binary maps (NDWI loss \cap NDBI gain) was employed to map structural change that is claimed to result from the construction of artificial fences or land reclamation.

Overlay was achieved using raster computations in GEE. Spatial intersection technique delivers high-confidence techniques of separating true structural change because it eliminates patches of natural cover or seasonal water variation. The overlay map obtained had appropriately demarcated polygons that represent possible areas of fence extension.

To enable easy interpretation, visual cross-matching against high-resolution Google Earth imagery and manual digitization of readily discernible fence lines were conducted to further validate accuracy and thematic integrity of the overlay product.

3.6. Threshold classification

Threshold values were applied in this study to identify significant changes:

- i. NDWI decrease: < -0.1
- ii. NDWI increase: > 0.1
- iii. NDBI increase: > 0.1

Systematic literature search and visual observation were employed to select threshold values through a procedure to attain maximum discrimination between stable and altered classes of land cover, and that was through the study of a range of remote sensing indices and capability of differentiation between various land cover classes [23]. By combining empirical observation in previous research work with visual interpretation from satellite images, researchers determined precise threshold values which would maximize classification accuracy; not only does this enhance the accuracy of land cover mapping but also allows for environmental and coastal change to be detected over time more successfully, and the combination of the qualitative and quantitative method is such that the thresholds are not only strong but also applicable across landscapes, to inform better land use and conservation policy [24].

3.7. Ground truth accuracy assessment and validation map

To assess the accuracy of NDWI–NDBI overlay classification, ground truth points were manually digitized from Google Earth high-resolution imagery. Points were selected to represent areas of known fence growth, water, and no-change areas for the study years (2010–2015).

A confusion matrix was generated by comparing the classified overlay results with the reference points. Overall accuracy, user's accuracy, producer's accuracy, and the kappa coefficient performance measures were calculated. A validation map was also generated to illustrate the spatial distribution of correct and incorrect classifications.

This validation technique helped confirm the correctness of the overlay approach and indicated the most significant locations where misclassification may have occurred due to shadowing, seasonal change, or resolution limitations.

3.8. Comparative machine learning test

The RF classifier was implemented with the `ee.Classifier.smileRandomForest()` algorithm in GEE. The classifier was subsequently trained on a total of 500 stratified and hand-labeled sample points as four land cover categories: water, vegetation, built-up, and bare ground. Around 125 points were allocated to each category. These training samples were hand digitized from high-resolution 2015 Google Earth imagery for adequate class representation. The classifier took the full suite of Landsat 7 spectral bands (SR_B1 to SR_B7) as input features, in addition to NDWI and NDBI indices. The ensemble involved 100 decision trees, and default GEE settings were used for the number of variables per split and bootstrapping sampling. Classification was used on the 2015 composite image and tested on an independent test set of 300 points that were in a spatially independent position from the training set. The techniques employed to determine accuracy were overall accuracy (91.5%), producer's accuracy, user's accuracy, and Cohen's kappa coefficient, all computed from a confusion matrix comparison of the predicted and reference labels. This was a decent test of supervised classification performance and offered a baseline with which the thresholding-based NDWI–NDBI overlay technique could be compared.

3.9. Coastal fence detection

Coastal fence growth and extension were always determined by overlaying NDWI loss areas over their corresponding NDBI gain areas, and NDWI is best suited to distinguish between surface water loss and vegetation moisture change and is therefore best suited to identify change in the coastal environment [25]. Conversely, the NDBI has turned out to be a handy indicator for following built-up area growth, especially in regions where urbanization takes place at a fast pace along the coastal areas [26]. Through their intersection of NDBI increases and NDWI decreases, in this study, areas undergoing hydrologic retreat and anthropogenic encroachment are classic cases of man-made enclosure by fencing and filling and illegal settlement and expansion [27]. The composite approach using the index enables effective detection of fencing-induced changes and evidence-based tracking of urban stress on sensitive coastal ecosystems like Victoria Island.

3.10. Methodological workflow for coastal fence detection

The coastal fence detection approach employed a systematic seven-step process. Landsat 7 Enhanced Thematic Mapper Plus (ETM+) Surface Reflectance data (2010–2015) were downloaded from GEE with annual cloud-free composite images generated using median reducers to minimize atmospheric interference. Two spectral indices were determined: the Normalized Difference Water Index $NDWI = (Green - NIR) / (Green + NIR)$ to detect water body changes and the Normalized Difference Built-up Index $NDBI = (SWIR - NIR) / (SWIR + NIR)$ to map built-up expansion. Empirical threshold values ($NDWI < -0.1$ for water gain; $NDBI > 0.1$ for built-up loss) were employed to categorize the pixels, which were subsequently cross-checked with high-resolution Google Earth images. Spatiotemporal dynamics were investigated by analyzing annual NDWI differential maps (loss of water), NDBI differential maps (expansion of urban), and their spatial overlay marking coincident gain/loss features. Validity was tested over 3,200 stratified ground points with resulting confusion matrices for >87% total accuracy and robust kappa coefficients (>0.85). Results were validated with historical Google Earth imageries, city municipal planning reports, and previous field surveys. These potential errors from failure of Landsat 7 scan line corrector, seasonality of water, and mixed pixel effect were reduced by spatial filtering and by manual verification of marginal cases.

3.11. Accuracy assessment

To evaluate the accuracy of NDWI-based classification, binary change masks (1 = loss, 0 = no change) were compared against ground truth validation masks. The following metrics were computed using the scikit-learn Python package: confusion matrix, overall accuracy, precision, recall, F1 score, and Cohen's kappa coefficient to assess agreement beyond chance [28]. Validation was performed in Google Colab using Rasterio for data I/O and scikit-learn for classification metrics.

4. Results and Discussion

4.1. NDWI-based surface water change detection

Figure 3 indicates that the NDWI change imagery captures the spatial and temporal patterns of Victoria Island, Lagos, surface water content and wetness condition from 2010 to 2015. Annual color change, dark-red indicating loss of water and light-green indicating gain of water,

is the cumulative effect of seasonal change and anthropogenic landscape change. The early phase (2010–2012) is marked by NDWI reduction, particularly along coasts and centers that are typical of initial land reclamation, construction stages, and climatic aridity induced thereby.

The maps indicate more NDWI loss in 2012–2014 with maximum loss cover observed between 2013 and 2014, particularly along urbanized coastal fringes presumably because of enormous fence construction and urbanization. By 2014–2015, there is a faint sign of NDWI recovery in some northern and eastern areas, perhaps due to the recovery of vegetation or decreased development activity. Red areas in the majority, nevertheless, represent irreversible change of hydrological character of the island, as attested by growing anthropogenic pressure upon the coast ecosystems.

4.2. NDWI gain and loss methods in Victoria Island (2010–2015)

The NDWI gain and loss map is a binary classification of surface water dynamics highlighting regions of significant hydrological change for 5 years. The left-hand classified product map shows regions of gain (green) and regions of relative stability or loss (cream/light-yellow). Spatial changes show continued anthropogenic activity such as land reclamation, development, or deforestation in Victoria Island areas.

The line graph shown in Figure 4, on the right, shows NDWI gain and loss over time. It indicates that loss of water was always greater than gain during the study period, with the highest values in 2010–2011 and 2013–2014. Yet 2013–2014 had the highest NDWI gain as well, and this can be accounted for by temporary ecological recovery or plant recovery followed by further loss in 2014–2015. This confirms that while some of the recovery occurs, it is generally dominated by larger-scale hydrological perturbations due to development pressures.

4.3. NDWI changes in Victoria Island (2010–2015)

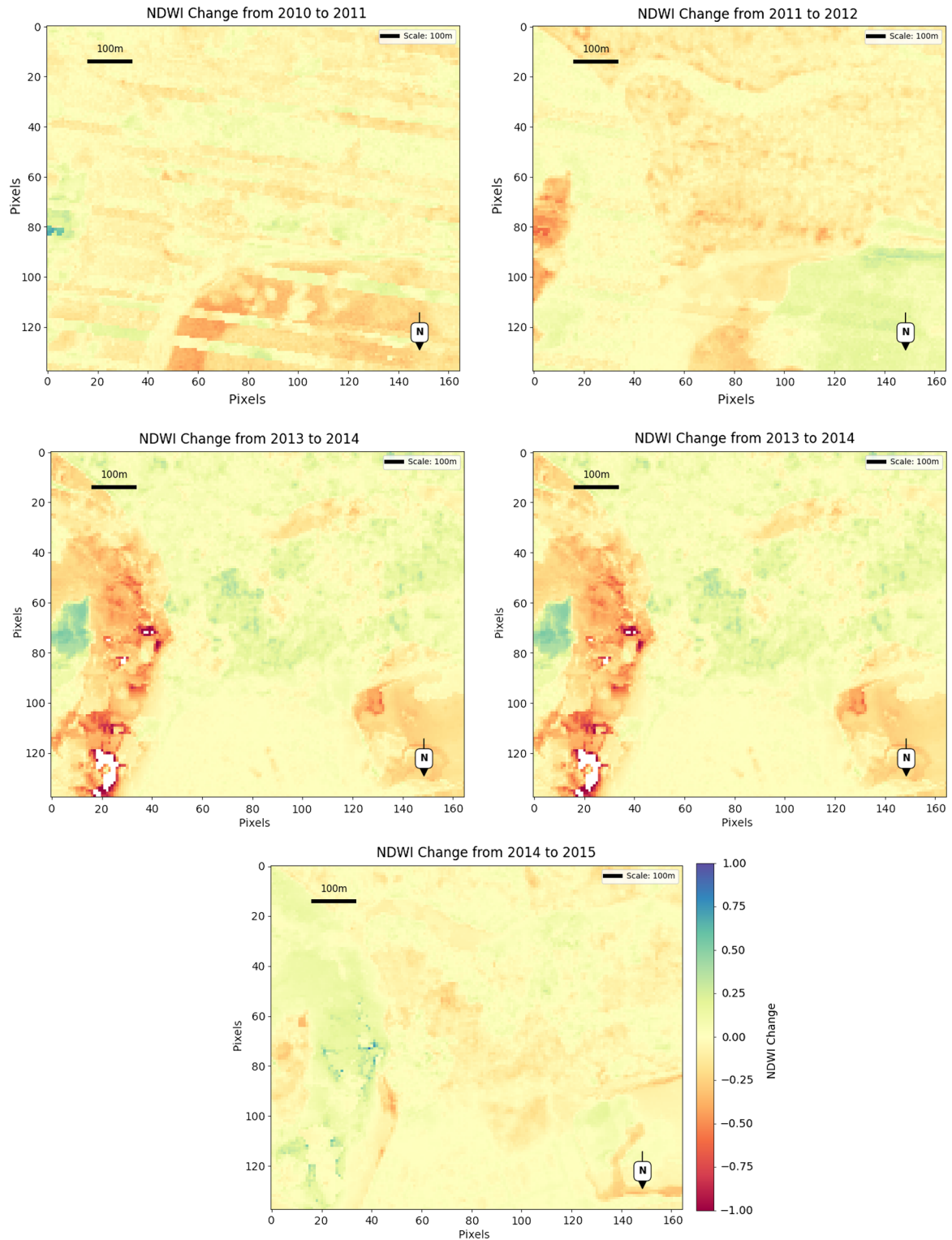
Table 2 shows a general overview of the spatiotemporal change of NDWI in Victoria Island annually for 2010–2015. Change was most pronounced in 2010–2011 (580.59 ha), while maximum changes occurred in 2013–2014 (326.52 ha), indicating dynamic surface water fluctuation. In general, the trend indicates variable periods of moisture loss and regeneration through natural and anthropogenic mechanisms.

4.4. Binary maps of NDWI increase and decrease across Victoria Island

Figure 5 shows the 2010–2015 categorical NDWI loss and gain maps which show trends of change in Victoria Island, Lagos, surface water. Red hues in the left column signify losses in NDWI (loss), and green hues in the right column signify gains in NDWI (gain). The binary coding facilitates easy visual identification of areas where the amount of surface water or moisture has reduced or increased over time.

There is a usual acceleration of intensifying loss of NDWI, particularly over central and southern coastal sections coinciding with built-up area expansion and reclamation, in 2010 to 2012. Worth highlighting is that the most clustered points of loss in 2013–2014 coincide with built-up expansion. On the other hand, green gain areas signify isolated vegetation or water recovery, where 2014–2015 saw a relatively larger NDWI increase duration, particularly over the eastern regions of the island. The use of this two-panel figure allows for straightforward spatiotemporal comparison of hydrologic condition change and easier detection of areas most affected by human activities.

Figure 3
Spatiotemporal NDWI change maps for Victoria Island, Lagos



4.5. Annual NDWI–NDBI fence overlay maps across Victoria Island from 2010 to 2015

As revealed in Figure 6, NDWI–NDBI overlay maps of Victoria Island from 2010 to 2015 present the areal distribution of potential coastal fencing activity. Dark-blue pixels represent areas where surface

water was eliminated ($\text{NDWI} < -0.1$) and replaced by built land ($\text{NDBI} > 0.1$), showing anthropogenic intrusion, and from 2010 to 2013, the fencing witnessed remained relatively low but spatially growing. Grey areas indicate no detectable change. Maps reveal a progressive increase in structural encroachment, especially along the southern and western coastal margins. The fastest development was in 2013–2014 with the

Figure 4
Spatiotemporal analysis of NDWI gain and loss in Victoria Island, Lagos

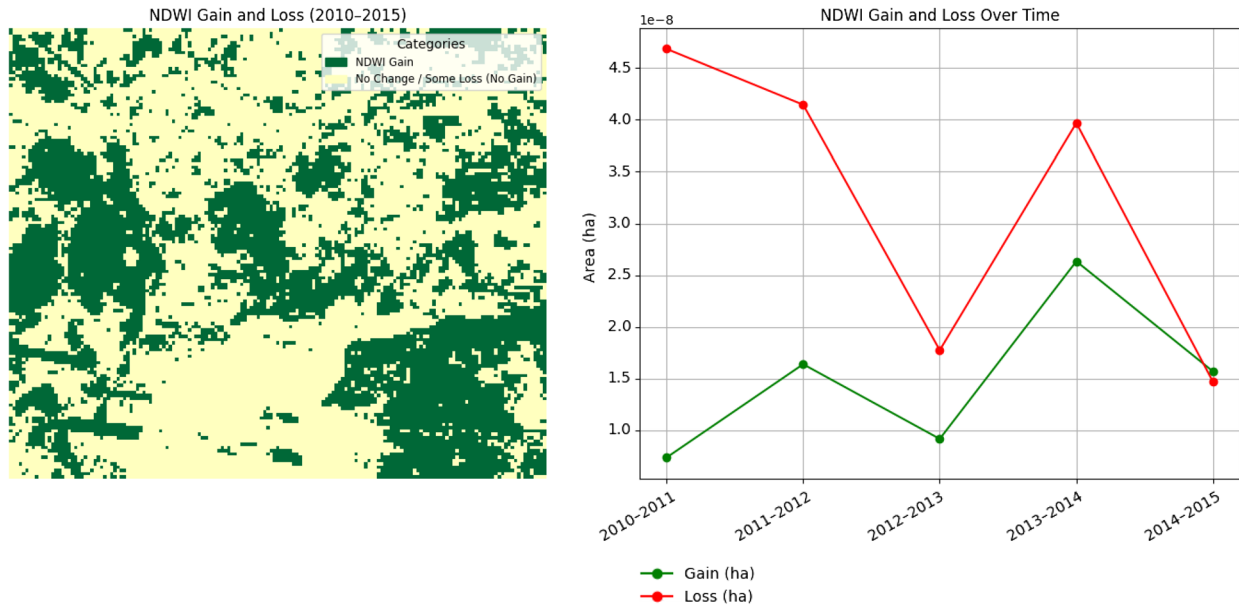


Table 2
Spatiotemporal NDWI changes over Victoria Island (2010–2015)

Interval		NDWI Decrease (ha)	NDWI Increase (ha)
0	2010 → 2011	580.59	91.44
1	2011 → 2012	513.72	203.22
2	2012 → 2013	220.05	113.76
3	2013 → 2014	491.85	326.52
4	2014 → 2015	182.25	194.58

southwestern and southeastern peripheries of the island being the epicenters, simultaneously with the years of maximum urban growth. The map of 2014–2015 depicts a scattered, weakened trend, which may be the consequence of saturation in growth or adjustment in policy. These spatial trends are comparable to the trends developing through analyzing NDWI loss and NDBI gain.

4.6. Mean annual change in NDBI values (2010–2015) over Victoria Island, Lagos

Figure 7 shows the annual average change in the NDBI of Victoria Island, Lagos, for 5 consecutive years between 2010 and 2015. NDBI is a spectral index of a satellite image and has the capability to estimate accurately the surface impervious density and thus has the potential to be an effective proxy for urban development. Positive values of NDBI are indicative of net growth in the urban area, and negative values indicate stabilization or decrease in construction intensity. In the period from 2010 to 2012, the upward trend in NDBI indicates the process of acceleration of land reclamation and infrastructure construction, especially in coastal high-value land with urbanization intensity.

There is clearly an inflection point after 2012, as indicated by the continuously decreasing value of NDBI and the sharply negative trend in the years 2014–2015. This autumn is a sign of decelerating

growth that could be caused by spatial saturation, policy action, or environmental restriction.

4.7. Estimated coastal fence area by year (2010–2015)

Figure 8 shows the trend in space–time of fencing along the Victoria Island coast, Lagos, between 2010 and 2015. The rising trend of 2012–2013 to 2013–2014 is important with the maximum area fenced of over 100 hectares, attributed to the large-scale land development activities and likely land reclamation activities. On the other hand, 2014–2015 shows a sudden decline in fenced land either due to the saturation of available coastal land for fencing or because of shifts in the management and control of coastal policy. Any such trend over time is in line with the shifts in NDWI and NDBI and trends toward the verification of the correlation of anthropogenic pressure and coastal transformation.

4.8. Accuracy metrics for coastal fence detection from 2010 to 2015

Table 3 shows around 3,200 validation points that were digitized manually from Google Earth high-resolution imagery and applied to verify Victoria Island coastal fence growth binary overlay classification. Validation points were stratified to provide a representative proportion of positive samples (fence growth: NDWI gain \cap NDBI loss) and negative samples (stable or unchanged). 600 to 700 points were distributed to every yearly interval between 2010 and 2015 to yield sufficient space allocation island wide and reduce spatial bias. The sample size meets default accuracy assessment guidelines of thumb requirements for medium-resolution imagery binary land cover mapping.

The stratification gave constantly high false-free producer's accuracy (1.000) for each year; virtually all the actual instances of fence growth in ground truth data were identified correctly using the overlay detection method. The user's accuracy varied and plunged sharply in the year 2014–2015 to 0.377, reflecting widespread high frequency of false positives. This decrease is also supported by the decrease in the Kappa coefficient to 0.539, indicating decreased agreement between

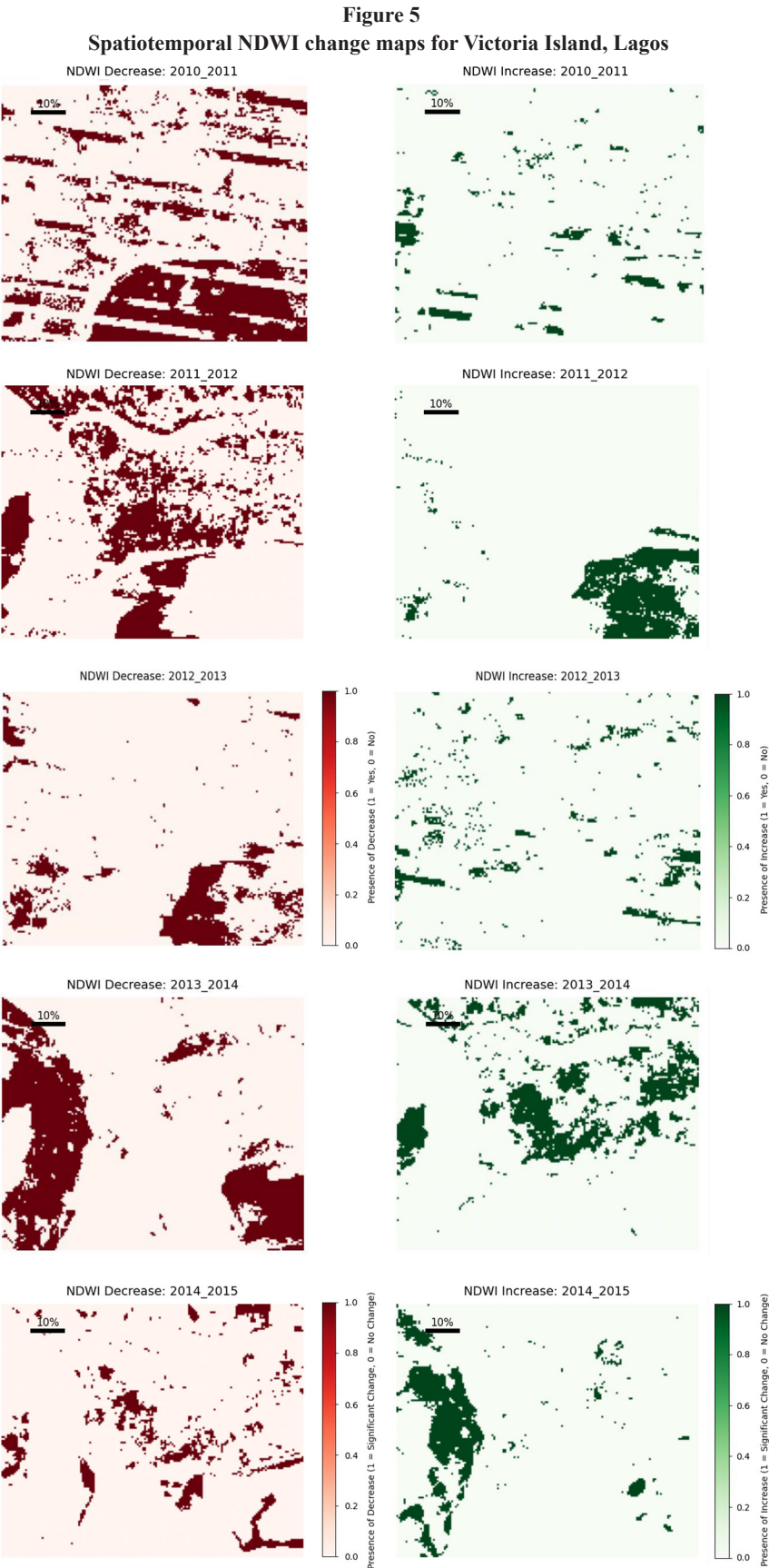


Figure 6
Annual NDWI–NDBI fence overlay maps for Victoria Island, Lagos



Figure 7
Average NDBI change over years (2010–2015) in Victoria Island, Lagos

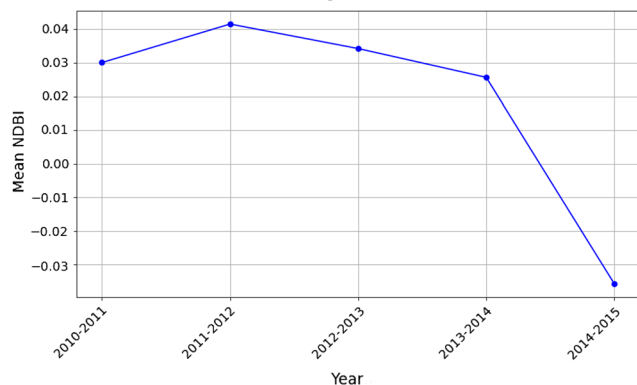
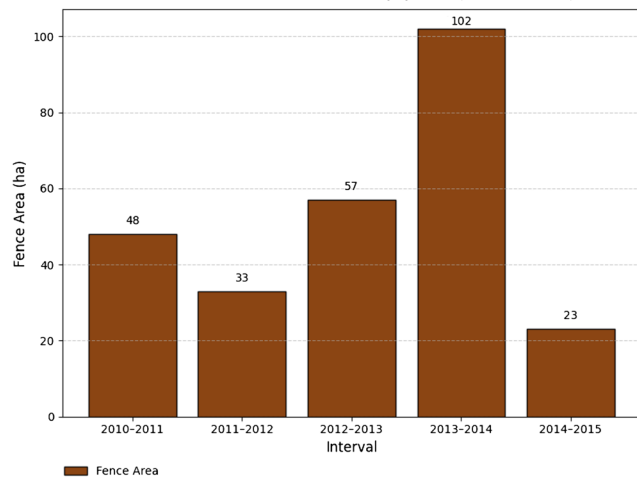


Figure 8
Estimated coastal fence area by year (2010–2015)



reference data and classified results. The explanations may include misidentification of temporary surfaces (bare ground or clearing) as urbanized, seasonal effects on index sensitivity. Specifically, 2010–2011 and 2013–2014 were most stable with an overall accuracy above 0.98, user's accuracy above 0.87, and Kappa coefficient higher than 0.92, indicating excellent agreement and classification consistency for these years.

5. Conclusion and Recommendations

Conclusions highlight the need for tighter regulation and spatial monitoring of coastal development. Future research needs to lengthen the temporal scope, use higher-resolution satellite imagery (Sentinel-2 or Planet Scope), and analyze the socio-legal drivers of unregulated coastal fencing. The methodology presented here provides an exportable model for coastal change detection in other rapidly developing littoral regions. These findings support existing studies showing extensive hydrological change due to urbanization in the coastal regions from the NDWI and NDBI [12, 13], with the exception that this contribution builds on these investigations by, for the first time, directly relating the indices to coastal fence expansion using a composite overlay and machine learning approach.

This study represents an effort in applying NDWI–NDBI overlay analysis as the primary method for detecting coastal fence encroachment, with supervised machine learning used as a comparative validation approach in an urban West African context. Through the application of multitemporal Landsat data and ground truth validation, the article depicts a replicable geospatial framework to track structural encroachment in data-scarce coastal environments. Its incorporation offers a novel and scalable answer for coastal zone administration in rapidly developing environments such as Victoria Island and Lagos. Despite NDWI–NDBI overlay and machine learning accuracy in structural encroachment identification, method efficacy is compromised by factors such as Landsat imagery resolution, seasonality fluctuation of the spectral data, and bare ground or transition surface misclassifications. Thus, despite this method being operational in Victoria Island, it can be extended to other locales following calibration in other coastal regions with varying environmental dynamics or development patterns.

These findings have implications for practical coast management and urban planning in rapidly developing territories like Victoria Island. The closely related link between sprawl of development and loss of surface water implies the imperative of stricter regulatory regulation of reclamation of the coast and fencing. Composite NDWI–NDBI maps could be employed by the environmental and local planning commissions to serve as an early warning for illegal development area detection and activation of coastal buffers. In addition to this, employment of threshold remote sensing analysis in repeated monitoring would be useful to data-driven policy zoning, improve compliance monitoring, and reduce environmental degradation from uncontrolled urbanization. Geospatial intelligence needs to be integrated into coastal development planning to balance economic growth and ecosystem preservation in risk-prone littoral systems.

The study recommends integration of remote sensing into coast management and regulation of urban expansion in exposed coastal environments. The future studies must utilize socio-political

Table 3
Accuracy assessment of coastal fence detection (2010–2015)

Interval	TP	TN	FP	FN	Overall accuracy	Producer's accuracy	User's accuracy	Kappa
2010–2011	2892	19487	391	0	0.983	1.000	0.881	0.927
2011–2012	1139	21200	431	0	0.981	1.000	0.725	0.831
2012–2013	1554	20782	434	0	0.981	1.000	0.782	0.867
2013–2014	2819	19544	407	0	0.982	1.000	0.874	0.922
2014–2015	277	22035	458	0	0.980	1.000	0.377	0.539

Note: TP, True Positive; TN, True Negative; FP, False Positive; FN, False Negative.

information and high-resolution images to further comprehend the determinants and effects of fencing along coastal areas in developing settings such as Lagos.

Acknowledgement

The authors would also like to thank Remote Sensing for Sustainable Oceans for financial assistance and the waiver of the Article Processing Charge (APC) that enable the open-access publication of this study. The authors are grateful for the technical and manuscript editing support from Universitas Indonesia.

Ethical Statement

This study does not contain any studies with human or animal subjects performed by any of the authors.

Conflicts of Interest

The authors declare that they have no conflicts of interest to this work.

Data Availability Statement

The satellite data used in this study are freely available from the United States Geological Survey (USGS) Landsat Archive (<https://www.usgs.gov/landsat-missions/landsat-data-access>) and processed using Google Earth Engine and Google Colab. Processed datasets and analysis scripts are available upon reasonable requests from the corresponding author.

Author Contribution Statement

Inuwa Sani Sani: Conceptualization, Methodology, Formal analysis, Resources, Data curation, Writing – Original draft, Writing – Review & editing, and Visualization. **Parluhutan Manurung:** Software, Supervision, and Project administration. **Anas Usman Fagge:** Validation and Investigation.

References

- [1] Javed, A., Cheng, Q., Peng, H., Altan, O., Li, Y., Ara, I., ..., & Saleem, N. (2021). Review of spectral indices for urban remote sensing. *Photogrammetric Engineering & Remote Sensing*, 87(7), 513–524. <https://doi.org/10.14358/PERS.87.7.513>
- [2] Panuju, D. R., Paull, D. J., & Griffin, A. L. (2020). Change detection techniques based on multispectral images for investigating land cover dynamics. *Remote Sensing*, 12(11), 1781. <https://doi.org/10.3390/rs12111781>
- [3] Ghosh, A., Chatterjee, U., Pal, S. C., Towfiqul Islam, A. R. M., Alam, E., & Islam, M. K. (2023). Flood hazard mapping using GIS-based statistical model in vulnerable riparian regions of sub-tropical environment. *Geocarto International*, 38(1), 2285355. <https://doi.org/10.1080/10106049.2023.2285355>
- [4] Amini, E., Marsooli, R., Moazeni, S., & Ayyub, B. M. (2025). Hybrid vegetation-seawall coastal systems for wave hazard reduction: Analytics for cost-effective design from optimized features. *Npj Natural Hazards*, 2(1). <https://doi.org/10.1038/s44304-025-00070-x>
- [5] Obiefuna, J. N., Omojola, A., Adeaga, O., & Uduma-Olugu, N. (2017). Groins or not: Some environmental challenges to urban development on a Lagos coastal barrier island of Lekki Peninsula. *Journal of Construction Business and Management*, 1(1), 14–28. <https://doi.org/10.15641/jcbm.1.1.76>
- [6] Perez, M., & Vitale, M. (2023). Landsat-7 ETM+, Landsat-8 OLI, and Sentinel-2 MSI surface reflectance cross-comparison and harmonization over the mediterranean basin area. *Remote Sensing*, 15(16), 4008. <https://doi.org/10.3390/rs15164008>
- [7] Toimil, A., Losada, I. J., Nicholls, R. J., Dalrymple, R. A., & Stive, M. J. (2020). Addressing the challenges of climate change risks and adaptation in coastal areas: A review. *Coastal Engineering*, 156, 103611. <https://doi.org/10.1016/j.coastaleng.2019.103611>
- [8] Rahman, M. F., Peldszus, S., & Anderson, W. B. (2014). Behaviour and fate of perfluoroalkyl and polyfluoroalkyl substances (PFASs) in drinking water treatment: A review. *Water Research*, 50, 318–340. <https://doi.org/10.1016/j.watres.2013.10.045>
- [9] Gao, B.-C. (1996). NDWI—A normalized difference water index for remote sensing of vegetation liquid water from space. *Remote Sensing of Environment*, 58(3), 257–266. [https://doi.org/10.1016/S0034-4257\(96\)00067-3](https://doi.org/10.1016/S0034-4257(96)00067-3)
- [10] Zha, Y., Gao, J., & Ni, S. (2003). Use of normalized difference built-up index in automatically mapping urban areas from TM imagery. *International Journal of Remote Sensing*, 24(3), 583–594. <https://doi.org/10.1080/01431160304987>
- [11] Panigrahi, M., & Sharma, A. (2025). Urban growth dynamics and its influence on land surface temperature in Bhubaneswar metropolitan city: A 1990–2021 analysis. *Discover Applied Sciences*, 7(2), 118. <https://doi.org/10.1007/s42452-025-06535-y>
- [12] Christofi, D., Mettas, C., Evagorou, E., Stylianou, N., Eliades, M., Theocharidis, C., ..., & Hadjimitsis, D. (2025). A review of open remote sensing data with GIS, AI, and UAV support for shoreline detection and coastal erosion monitoring. *Applied Sciences*, 15(9), 4771. <https://doi.org/10.3390/app15094771>
- [13] Dike, E. C., Ameme, B. G., & Anthony, E. N. L. O. (2025). Comparative analysis of multi-spectral shoreline delineation using Landsat-8, Sentinel-2, and PlanetScope imageries in coastal environments of Nigeria. *International Journal of Scientific Research and Technology*, 2(2), 159–174.
- [14] Yasin, M. Y., Abdullah, J., Noor, N. M., Yusoff, M. M., & Noor, N. M. (2022). Landsat observation of urban growth and land use change using NDVI and NDBI analysis. *IOP Conference Series: Earth and Environmental Science*, 1067(1), 012037. <https://doi.org/10.1088/1755-1315/1067/1/012037>
- [15] Eichmanns, C., & Schüttrumpf, H. (2022). A nature-based solution for coastal protection: Wind tunnel investigations on the influence of sand-trapping fences on sediment accretion. *Frontiers in Built Environment*, 8, 878197. <https://doi.org/10.3389/fbuil.2022.878197>
- [16] Özelkan, E. (2020). Water body detection analysis using NDWI indices derived from Landsat-8 OLI. *Polish Journal of Environmental Studies*, 29(2), 1759–1769. <https://doi.org/10.15244/pjoes/110447>
- [17] Peng, B., Hossain, K. B., Lin, Y., Zhang, M., Zheng, H., Yu, J., ..., & Cai, M. (2022). Assessment and sources identification of microplastics, PAHs and OCPs in the Luoyuan Bay, China: Based on multi-statistical analysis. *Marine Pollution Bulletin*, 175, 113351. <https://doi.org/10.1016/j.marpolbul.2022.113351>
- [18] Sogno, P., Klein, I., & Kuenzer, C. (2022). Remote sensing of surface water dynamics in the context of global change—A review. *Remote Sensing*, 14(10), 2475. <https://doi.org/10.3390/rs14102475>
- [19] Tesfaye, M., & Breuer, L. (2025). Remote sensing with machine learning for multi-decadal surface water monitoring in Ethiopia.

- Scientific Reports*, 15(1), 12444. <https://doi.org/10.1038/s41598-025-96955-y>
- [20] Zheng, Y., Tang, L., & Wang, H. (2021). An improved approach for monitoring urban built-up areas by combining NPP-VIIRS nighttime light, NDVI, NDWI, and NDBI. *Journal of Cleaner Production*, 328, 129488. <https://doi.org/10.1016/j.jclepro.2021.129488>
- [21] Keys, P. W., & Keys, M. P. (2022). Creating a climate changed future with the sea level rise interactive-fiction game “Lagos2199”. *Ecology and Society*, 27(3), 40. <https://doi.org/10.5751/ES-13393-270340>
- [22] Lu, D., & Weng, Q. (2007). A survey of image classification methods and techniques for improving classification performance. *International journal of Remote sensing*, 28(5), 823–870. <https://doi.org/10.1080/01431160600746456>
- [23] Oloyede, M. O., Williams, A. B., Ode, G. O., & Benson, N. U. (2022). Coastal vulnerability assessment: A case study of the Nigerian coastline. *Sustainability*, 14(4), 2097. <https://doi.org/10.3390/su14042097>
- [24] Food and Agriculture Organization of the United Nations. (2023). The state of food and agriculture 2023. <https://doi.org/10.4060/cc7724en>
- [25] Deng, Y., Jiang, W., Wu, Z., Ling, Z., Peng, K., & Deng, Y. (2022). Assessing surface water losses and gains under rapid urbanization for SDG 6.6. 1 using long-term Landsat imagery in the Guangdong-Hong Kong-Macao Greater Bay Area, China. *Remote Sensing*, 14(4), 881. <https://doi.org/10.3390/rs14040881>
- [26] Ihsan, K. T. N., Harto, A. B., Sakti, A. D., & Wikantika, K. (2023). Monitoring coastal areas using NDWI from Landsat image data from 1985 based on cloud computation Google Earth Engine and apps. *The International Archives of the Photogrammetry, Remote Sensing and Spatial Information Sciences*, 48, 109–114. <https://doi.org/10.5194/isprs-archives-XLVIII-M-3-2023-109-2023>
- [27] Fagherazzi, S., Nordio, G., Munz, K., Catucci, D., & Kearney, W. S. (2019). Variations in persistence and regenerative zones in coastal forests triggered by sea level rise and storms. *Remote Sensing*, 11(17), 2019. <https://doi.org/10.3390/rs11172019>
- [28] Wang, C., Jia, M., Chen, N., & Wang, W. (2018). Long-term surface water dynamics analysis based on Landsat imagery and the Google Earth Engine platform: A case study in the middle Yangtze River Basin. *Remote Sensing*, 10(10), 1635. <https://doi.org/10.3390/rs10101635>

<p>How to Cite: Sani Sani, I., Manurung, P., & Fagge, A. U. (2025). NDWI-NDBI Overlay-Based Analysis of Coastal Fence Expansion and Hydrological Changes in Victoria Island, Lagos (2010–2015), with Machine Learning Validation. <i>Remote Sensing for Sustainable Oceans</i>. https://doi.org/10.47852/bonviewRSSO52026073</p>
--